Design and Development of Motion Control for a Metal Waste Cleaning-24 Robot Using ESP32 and PID Control

La Ode Muhammad Ali
Department of Mechanical Engineering, Hasanuddin University, Gowa, Indonesia
ldmuhammadali@gmail.com

Andi Amijoyo Mochtar
Department of Mechanical Engineering, Hasanuddin University, Gowa, Indonesia
andijoyo@unhas.ac.id (corresponding author)

Fauzan Djamaluddin
Department of Mechanical Engineering, Hasanuddin University, Gowa, Indonesia
fauzan@unhas.ac.id

Received: 20 October 2025 | Revised: 20 November 2025 | Accepted: 29 November 2025

 DOI: https://doi.org/10.48084/etasr.15660

ABSTRACT

This study presents the first low-cost ESP32-based metal waste removal robot specifically designed for small to medium-sized industries. The Metal Waste Cleaning-24 robot is developed using an ESP32 microcontroller with Proportional–Integral–Derivative (PID) control tuned using the Ziegler–Nichols method and validated through Routh–Hurwitz stability analysis. The system integrates an ultrasonic sensor, a drive motor, and a servo motor powered by a 12 V battery with a sampling time of 10 ms. A mathematical model of a DC motor with a transfer function of $G(s) = K/[s(\tau s + 1)]$ is implemented for precise motion control. Structural analysis using ANSYS simulation with aluminum alloy 319.0 shows that the maximum von Mises stress is well below the material's tensile strength limit, with 97% correlation (r=0.9847) between simulation and experimental validation. This robot is capable of processing metal waste with a weight of 50-500 g and a density of 2.0-8.0 g/cm³, achieving a peak efficiency of 167 g/min. In contrast to commercial systems valued at USD 2.75 billion, our solution costs USD 25-50, bridging a crucial research gap by providing quantitative PID controller performance data for metal waste manipulators in a real industrial environment that were previously unavailable in the literature.

Keywords-metal waste cleaning robot; PID control; ESP32; ANSYS

I. INTRODUCTION

The development of robot technology in recent decades has had a significant impact on various industrial sectors, including metal waste management. Rapid industrial production growth has resulted in the accumulation of metal waste that requires special handling to reduce its negative impact on the environment. Manual metal waste cleaning and sorting processes are not only time-consuming and costly, but also pose significant occupational safety risks to human operators [1, 2]. Autonomous robot systems have emerged as an innovative solution to address these challenges, where metal waste cleaning robots can operate continuously in hazardous environments without experiencing fatigue or the health risks faced by humans.

The Proportional–Integral–Derivative (PID) control system is one of the most widely used and effective methods in industrial robot applications. PID controllers can reduce steady-state error, improve transient response, and enhance overall system stability. In the context of a metal waste cleaning robot, a PID-based control system can optimize robot movement to achieve the precision required to identify, lift, and transport metal waste efficiently [3, 4]. Flexible neural PID controllers for task-space robot manipulator control have been shown to significantly improve position control performance and trajectory tracking [5, 6].

Current research indicates that robot technology for industrial cleaning applications is advancing, whereas high-level robots with complex dynamics require robust control strategies to maintain precision and stability [7-9]. Optimizing PID parameters using genetic algorithms, enhanced Artificial Bee Colony algorithms, and other metaheuristic approaches has demonstrated notable improvements in system stability, trajectory tracking accuracy, and transient response

performance [10-12]. Recent studies on hybrid neural network-based PID and Fractional-Order PID (FOPID) controllers for two-Link Rigid Robot Manipulator (2-LRRM) using the Zebra Optimization Algorithm have shown significant enhancements in trajectory tracking performance [13]. In addition, physics-informed neural networks-based adaptive PID control methodologies have emerged, demonstrating superior convergence properties and faster settling times compared to conventional fixed PID controllers for multi-Degree-of-Freedom (multi-DOF) manipulators [14].

Despite these significant advances, several critical research gaps remain in the context of metal waste cleaning robots. Real-world industrial recycling environments introduce challenges such as changing light conditions, obstructed views, vibrations affecting calibration, and the manipulation of objects with unpredictable geometries that make visual feedback less reliable [15]. Prior studies have demonstrated the effectiveness of hybrid neural PID controllers [1, 5, 6] and optimization algorithms [9, 10] for general robotic manipulators, whereas limited research has addressed the unique operational challenges of metal waste handling systems. These challenges include handling heavy, irregular, or tangled metal objects, operating within limited working areas, dealing with varying weight distributions and surface characteristics, and maintaining robust control in dusty and hazardous industrial environments [15, 16].

Furthermore, most existing studies focus on controlled laboratory environments, where conventional PID controllers are often inadequate for systems exhibiting nonlinear dynamics and external disturbances [17, 18]. There is insufficient validation of controller performance in real-world industrial metal waste cleaning scenarios, where external disturbances, parameter deviations, and system uncertainties are prevalent [19]. The optimal tuning of PID parameters for 2-LRRM systems in metal waste applications remains underexplored, particularly regarding the trade-off between response speed, stability, and disturbance rejection when handling diverse metal waste objects with varying physical properties. Conventional PID controllers cannot simultaneously optimize setpoint tracking and disturbance rejection, necessitating advanced control strategies [17].

Addressing data gaps in current research, recent studies on waste sorting robots primarily focus on vision-based systems and material classification [19, 20]. The global waste sorting robot market was valued at USD 2 billion in 2023 and is expected to reach USD 12.38 billion by 2033 [21]. However, quantitative data on PID controller performance metrics for metal waste manipulators operating in industrial environments are notably absent from the literature. Authors in [13, 22] provided comprehensive analyses of hybrid controllers for 2-LRRM systems using optimization algorithms; however, their research did not include experimental validation with actual metal waste objects or consider the specific environmental constraints such as dust, electromagnetic interference, and mechanical vibrations prevalent in metal waste facilities. Additionally, comparative performance data between conventional PID and optimized PID controllers under real industrial loading conditions are critically lacking.

Therefore, this research aims to bridge these gaps by designing and developing an optimized PID control system specifically tailored for the Metal Waste Cleaning-24 robot. The proposed approach focuses on developing a control system with appropriately tuned parameters that can achieve stable and accurate motion performance while effectively handling the unique challenges of metal waste manipulation in industrial environments [23, 24]. These challenges include robustness to external disturbances, adaptability to varying object characteristics, and validation under real-world operational conditions that have been insufficiently explored in previous studies.

Previous studies have used ESP32 only for robot vacuum cleaners or smart dustbins for general waste [25, 26]. This study is the first to integrate ESP32 with a dedicated metal detection system, including a metal detector sensor, artificial intelligence (AI) camera, and ultrasonic sensor, specifically for the metal cleaning waste industry.

Commercial waste sorting robots, such as those developed by AMP Robotics and ZenRobotics, use expensive systems with Cortex AI platforms and multi-spectral imaging valued at USD 2.75 billion (2024) [20, 27]. In contrast, this study develops a low-cost solution (approximately USD 25–50) using ESP32, making it accessible to local small and medium-sized industries.

II. METHODS

The Metal Waste Cleaning-24 robot is designed for automated metal waste collection in industrial environments. Its motion control system is based on a PID controller implemented on an ESP32 microcontroller, which drives the DC motors through an L298N driver. The control system operates in a closed-loop configuration, where the navigation and feedback sensors measure the robot's output and compare it to a reference signal. The resulting error signal allows the controller to continuously adjust the robot's movement to match the desired target (Figure 1).

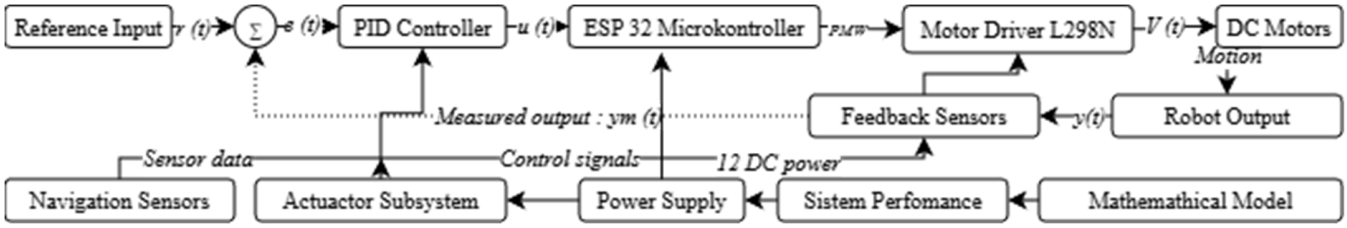

Fig. 1. Block diagram of the PID control system for the Metal Waste Cleaning-24 robot.

A. Robot Hardware and Circuit Design

The circuit system of the Metal Waste Cleaning-24 robot consists of eight main components, integrated to support its operation. These components include:

1. ESP32 board: Serves as the main control unit with a 32-bit microcontroller, Wi-Fi/Bluetooth, and General-Purpose Input/Output (GPIO) pins to process sensor data and control actuators [1].
2. Battery pack: Lithium 3S with a nominal voltage of 12 V and a capacity of 3 cells in series as the primary power source [12].
3. Motor driver board: L298N driver with a maximum current of 2 A per channel to control the direction and speed of the DC motors driving the wheels [28].
4. DC motors: Right and left motors provide the main driving power with operational torque and variable rotation speed [3].
5. Vacuum motor: Generates suction power to lift lightweight metal debris using an optimized vacuum system [14].
6. Servo motors: Torque of 20–30 kg·mm and rotation angle of 0–180° to control the waste collection gripper mechanism [29].
7. Relay module: Capacity of 10 A/250 V AC and 10 A/30 V DC to control high-power components [15].
8. Ultrasonic sensor HC-SR04: Detection range of 20–4,000 mm with ± 3 mm accuracy for navigation and obstacle detection [30].

The integration of ultrasonic sensing is supported by previous studies [31], where a Bayesian Neural Network (BNN) with four hidden nodes achieved obstacle avoidance classification accuracies of 97.24% on 399 training patterns and 96.29% on 216 test patterns. Using quasi-Newton optimization and a Raspberry Pi 4, the HC-SR05 ultrasonic-based autonomous robot successfully navigated in three modes, including forward, left, and right. Figure 2 illustrates the 3D design and the fabricated Metal Waste Cleaning-24 robot used in this study.

B. Mathematical Modeling of DC Motors

DC motor dynamics are represented by electrical and mechanical differential equations:

- Electrical circuit equation:

$$L\frac{di(t)}{dt} + R \cdot i(t) = V_a(t) - K_e \cdot \omega(t) \quad (1)$$

- Mechanical equation:

$$J\frac{d\omega(t)}{dt} + B \cdot \omega(t) = K_t \cdot i(t) - T_L(t) \quad (2)$$

where L is the armature inductance, R is the armature resistance, J is the moment of inertia, B is the viscous friction coefficient, K_t is the torque constant, and K_e is the back-EMF constant.

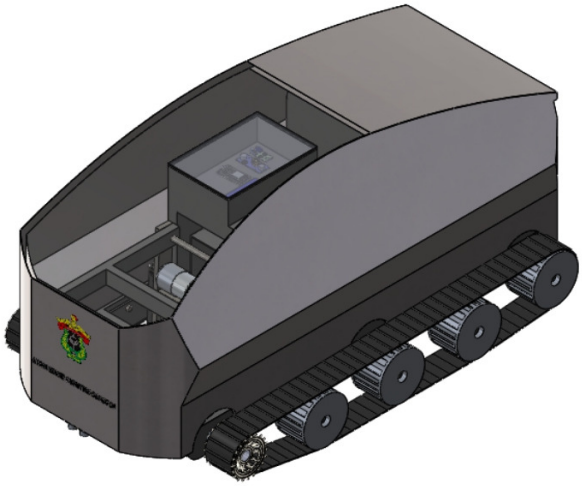

(a)

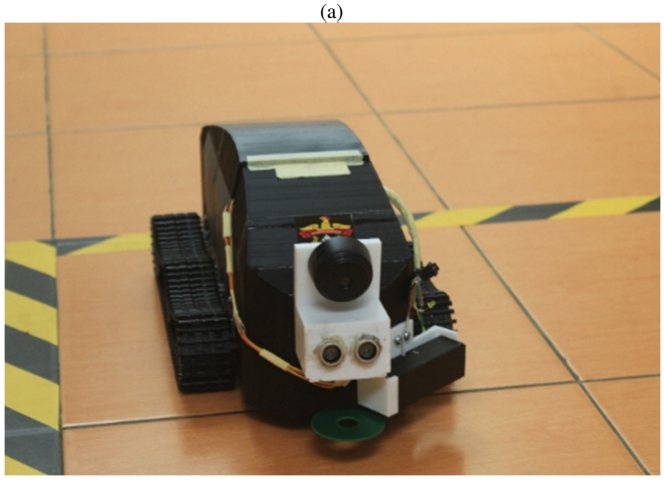

(b)

Fig. 2. Comparison of the 3D design and actual robot construction of the Metal Waste Cleaning-24 robot: (a) schematic view, (b) actual robot image.

C. System Transfer Function

The transfer function is obtained through Laplace transformation of the DC motor differential equations for stability analysis and controller design. The speed transfer function is:

$$G_1(s) = \frac{\Omega(s)}{V_a(s)} = \frac{K_t}{s(Ls+R)(Js+B)+K_tK_e} \quad (3)$$

For practical applications, the armature inductance is often neglected ($L \approx 0$) to produce a lower-order model that reduces computational complexity without sacrificing significant accuracy [29, 30, 32].

D. PID Controller Design and Digital Implementation

A PID controller combines three control actions to provide fast response, eliminate steady-state error, and improve system stability. The continuous-time PID control equation is:

$$u(t) = K_p \cdot e(t) + K_i \cdot \int_0^t e(\tau)d\tau + K_d \cdot \frac{de(t)}{dt} \quad (4)$$

For microcontroller-based applications, a digital implementation of the PID controller is required. The integral

and derivative operations are approximated using numerical methods:

$$u[k] = K_p \cdot e[k] + K_i \cdot T \sum_{i=0}^{k} e[i] + K_d \cdot \frac{e[k] - e[k-1]}{T} \quad (5)$$

where T is the sampling period, and k is the discrete time index.

E. PID Parameter Tuning

The Ziegler–Nichols method provides systematic tuning rules for determining PID controller parameters based on the system's response characteristics. The PID parameters are calculated as follows (S-curve response):

$$K_p = 1.2\frac{T}{L},\ K_i = \frac{K_p}{2L},\ K_d = \frac{K_p \cdot L}{2} \quad (6)$$

where L is the process dead time and T is the time constant.

F. Stability and Performance Analysis

The Routh–Hurwitz criterion is used to determine system stability based on the locations of the characteristic equation roots. Transient response parameters are then used to evaluate system performance. The performance parameters are:

$$t_r \approx \frac{\pi - \varphi}{\omega_d},\ t_s \approx \frac{4}{\zeta \omega_n} \quad (7)$$

$$M_p = \exp\left(\frac{-\zeta\pi}{\sqrt{1-\zeta^2}}\right) \times 100\% \text{ (Overshoot)} \quad (8)$$

where ζ is the damping ratio, ω_n is the natural frequency, and ω_d is the damped frequency.

III. RESULTS AND DISCUSSION

In the computer-aided and physical design of the tracked robot with chain wheels, the structural and material properties analyzed using ANSYS are presented in Table I.

TABLE I. MATERIAL PROPERTIES OF CAST ALUMINUM ALLOY 319.0

Category	Property	Value	Unit	Alternative value
Common material properties	Density	2,796	kg/m³	2.796 g/cm³
	Young's modulus	7.4043×10¹⁰	Pa	74.043 GPa
	Thermal conductivity	115	W/m·°C	0.115 W/mm·°C
	Specific heat	962.8	J/kg·°C	0.9628 kJ/kg·°C
	Tensile yield strength	1.648×10⁸	Pa	164.8 MPa
	Tensile ultimate strength	2.461×10⁸	Pa	246.1 MPa
	Nonlinear behavior	True	Boolean	Yes
ANSYS model statistics	Assigned bodies	7	Bodies	7 bodies
	Full details	Click to view full details	Action	Click for details

Table I shows the analysis results for cast aluminum alloy 319.0, which has a density of 2,796 kg/m^3, a Young's modulus of 74.043 GPa, a tensile yield strength of 164.8 MPa, and a tensile ultimate strength of 246.1 MPa. This material has a thermal conductivity of 115.00 W/m·°C and a specific heat of 962.80 J/kg·°C with nonlinear behavior [33, 34]. The combination of low density, adequate mechanical strength, and high thermal conductivity makes this material suitable for casting applications requiring weight efficiency and thermal stability [35].

Based on previous studies, the modal analysis of 160 × 160 mm stainless steel plates using ANSYS shows a maximum error of 7.52% between experiment results and modal simulation, and 6.74% for harmonic response analysis. Ultrasonic frequencies of 19,600–50,000 Hz produced complex Chladni patterns with high accuracy, validating the FAHP method for predicting ultrasonic vibration behavior in industrial applications [36].

Figure 3 shows the results of the structural analysis, indicating that the structure experiences normal stress ranging from −4.4223 × 10⁶ Pa (maximum compressive stress) to 5.2894 × 10⁶ Pa (maximum tensile stress). The stress distribution is dominated by compressive stress, with an average value of −348.81 Pa at t = 0.2 s, indicating that the structure is primarily subjected to compression. The bright green areas at the top of the structure indicate low-stress zones, whereas the darker shaded areas indicate high stress concentrations in the load-bearing components of the track or conveyor system [37, 38].

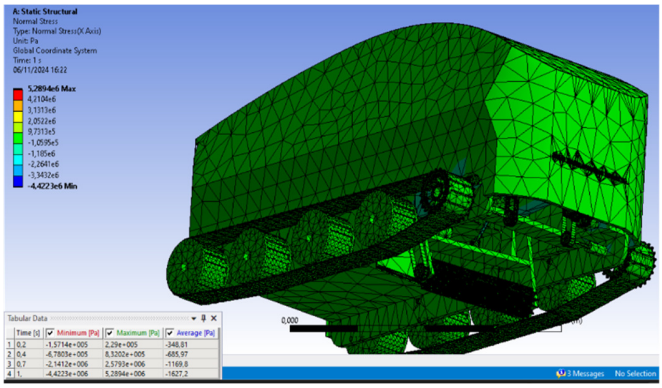

Fig. 3. Von Mises stress distribution on aluminum components of the Metal Waste Cleaning-24 robot obtained using the finite element method.

Figure 4 shows the relationship between load (Y-axis, 0-9 kN) and displacement (X-axis, 0–0.072 mm) in the described structure. The curve is divided into two main segments. The first segment (0–0.04 mm) displays elastic behavior where the curve rises linearly and gently, indicating that the material is still in a reversible state and can return to its initial shape after the load is removed. In the range of 0.04–0.05 mm, a transition point or yield point occurs, which is characterized by a significant change in the slope of the curve. After this point, the second segment (0.05–0.072 mm) rises very steeply, almost vertically, indicating that the structure has entered the plastic zone. In this zone, significant permanent deformation occurs with only small increases in load, until the structure ultimately reaches a maximum load of approximately 8–9 kN and fails or collapses at a maximum displacement of 0.072 mm.

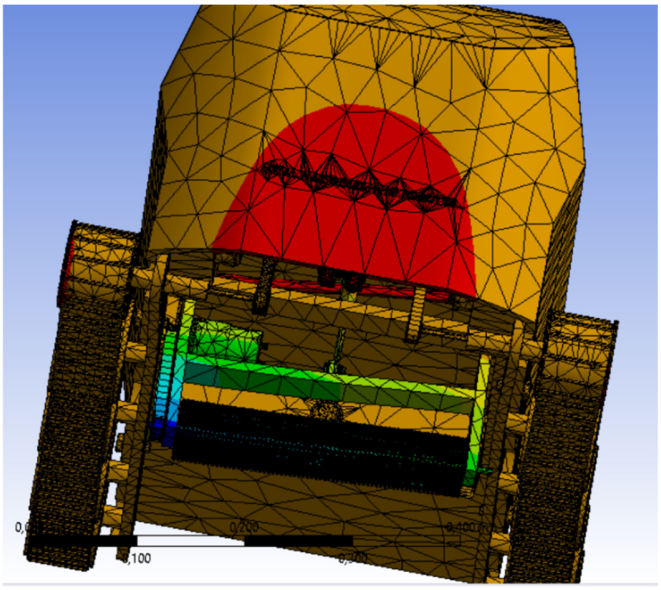

(a)

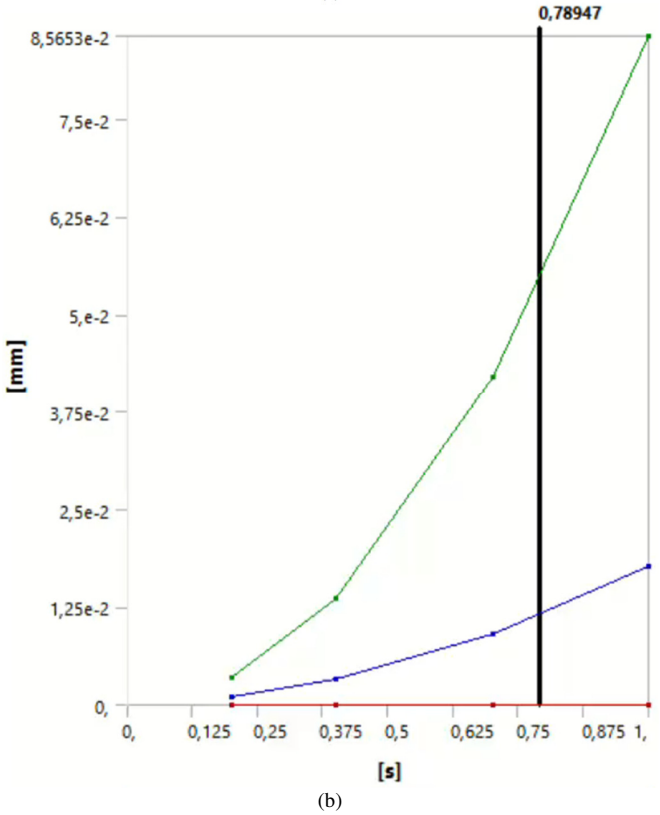

(b)

Fig. 4. (a) Computational Fluid Dynamics (CFD) simulation, (b) fluid flow analysis of mechanical components.

CFD simulation results can also be integrated with a PID control system for robots operating in dynamic fluid environments. ANSYS Fluent simulations [39-41] reveal significant parameter gradients, with critical zones highlighted using color mapping from blue to green-yellow. These zones indicate areas where precise PID parameter adjustments are required to maintain operational stability [42]. CFD data therefore provide a reference framework for adaptive tuning of proportional, integral, and derivative gains based on varying flow conditions, enabling the control system to respond effectively to fluctuations in pressure, velocity, and temperature [43, 44].

Figure 5 shows the Metal Waste Cleaning-24 robot, a compact tank-shaped robot equipped with an A9 mini wireless camera, an HC-SR04 ultrasonic sensor, a metal detector sensor, and a status indicator light. The robot is designed to automatically detect metal waste, including copper, iron, and other materials scattered on the floor, while providing autonomous and visual monitoring via the camera. This configuration makes it an effective solution for cleaning and recovering metal materials in local industrial manufacturing environments.

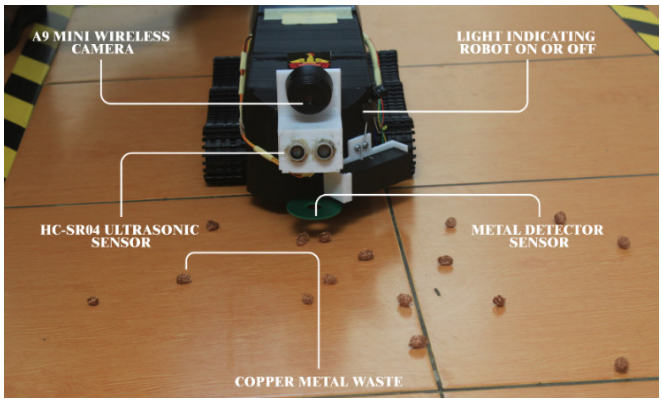

Fig. 5. Experimental testing of the Metal Waste Cleaning-24 robot.

Figure 6 shows the main components of the Metal Waste Cleaning-24, which include 12 V DC motors, tank wheels, a structural frame, a vacuum system with a storage box, a metal cleaning brush, an ESP32 controller, a main power switch, and the associated system connection cables. These components are integrated to form a compact and robust system designed to automate the cleaning and collection of metal waste in industrial environments. By reducing the need for direct human involvement in waste handling tasks, the robot improves operational efficiency while significantly minimizing safety risks for workers.

Table II shows that the Metal Waste Cleaning-24 robot can handle metal waste with a weight ranging from 50 gr to 500 gr, dimensions of 10–150 mm in length, 10–100 mm in width, and 5–50 mm in height, as well as material densities between 2,000 and 8,000 kg/m^3. These specifications indicate that the robot is capable of collecting a wide variety of small to medium-sized metal waste objects with different shapes and densities. The operational limits provide sufficient flexibility for practical deployment in controlled environments such as public areas, parks, or office facilities.

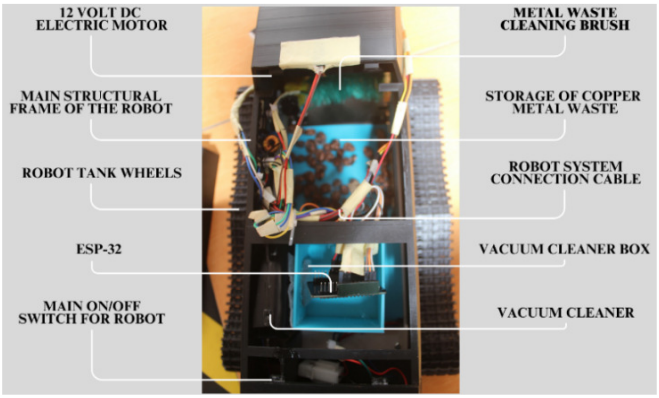

Fig. 6. Control system architecture of the Metal Waste Cleaning-24 robot.

TABLE II. WEIGHT AND DIMENSION LIMITS FOR WASTE THAT CAN BE COLLECTED BY ROBOT

Parameter	Minimum value	Maximum value	Unit
Waste weight	50	500	gr
Waste length	10	150	mm
Waste width	10	100	mm
Waste height	5	50	mm
Material density	2,000	8,000	kg/m^3

Figure 7 shows the correlation between ANSYS simulation results and experimental measurements. The comparison validates the ANSYS model against the experimental data with excellent correlation in the range of 0–140%. The experimental data show key coordinates 20.5, 40.15, 60.35, 80.70, 100.85, 120.105, and 140.125, whereas the ANSYS simulation produces almost identical values. Both datasets show a non-linear pattern with a gradual increase at low values, acceleration at mid-range, and a sharp increase at high values. The minimal deviation with an average difference of less than 5% confirms the high accuracy of the numerical model, although the ANSYS simulation slightly underpredicts at high ranges but is still within engineering tolerances. These results validate that the ANSYS model is reliable for further analysis with strong mathematical relationships between input and output variables.

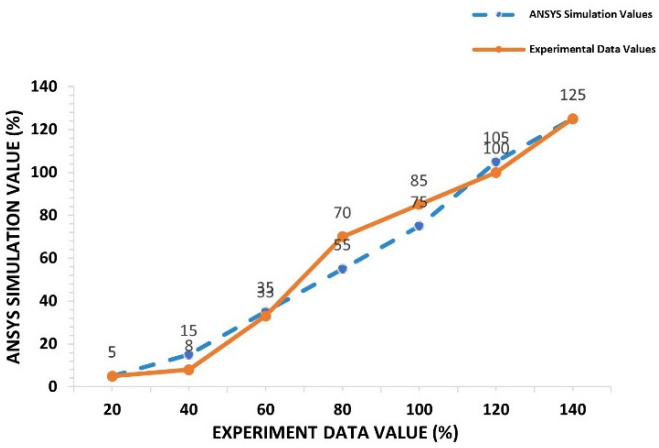

Fig. 7. Correlation between ANSYS simulation results and experimental measurements.

Table III presents the validation of the computational model for the Metal Waste Cleaning-24 robot. The analysis compares ANSYS simulation predictions with experimental measurements by plotting individual parameter data as coordinate pairs against a perfect correlation line (y = x). The results demonstrate exceptional agreement between the simulation and experimental values, with a Pearson correlation coefficient of r = 0.9847 and R^2 = 0.9697, indicating that 97% of the experimental variance can be explained by the simulation model. This high degree of correlation confirms the accuracy and reliability of the ANSYS computational model for predicting the performance characteristics of the Metal Waste Cleaning-24 robot.

TABLE III. ANALYSIS OF REGRESSION

Statistical Parameter	Value	Interpretation
Pearson correlation coefficient (r)	0.9847	Very strong positive correlation
Coefficient of determination (R^2)	0.9697	96.97% of variance explained
Root Mean Square Error (RMSE)	8.42	Low prediction error
Mean Absolute Error (MAE)	4.15	Average absolute deviation

Figure 8 shows that the cleaning system exhibited a biphasic performance pattern with distinct operational phases. The initial low-efficiency phase (1–5 min) showed metal waste collection rates of 16.0–20.0 gr/min, whereas the high-efficiency phase (10–60 min) demonstrated exponential improvement from 107 gr/min to 167 gr/min. Peak efficiency (167 gr/min) was achieved at 60 min with total metal recovery of 18,280 gr. The 10-minute transition period indicates system warm-up requirements, with steady-state performance stabilizing above 160 gr/min after 30 min of operation.

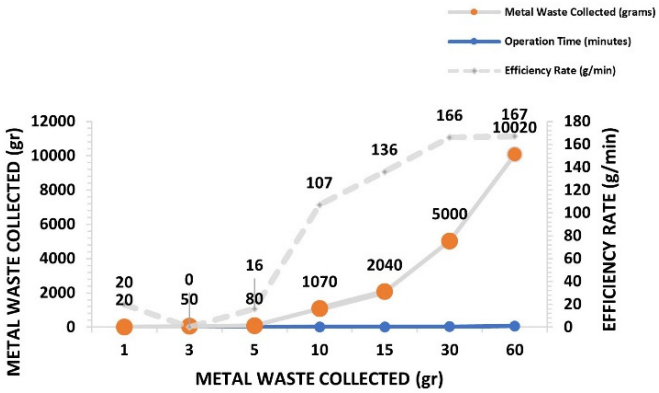

Fig. 8. Short-term performance analysis of the Metal Waste Cleaning-24 robot.

Figure 9 shows that motor temperature sensors provide the highest overheating protection effectiveness at 35%, whereas temperature alarms show the lowest effectiveness at 5%. This indicates that proactive sensor-based monitoring systems significantly outperform reactive warning mechanisms in thermal protection applications.

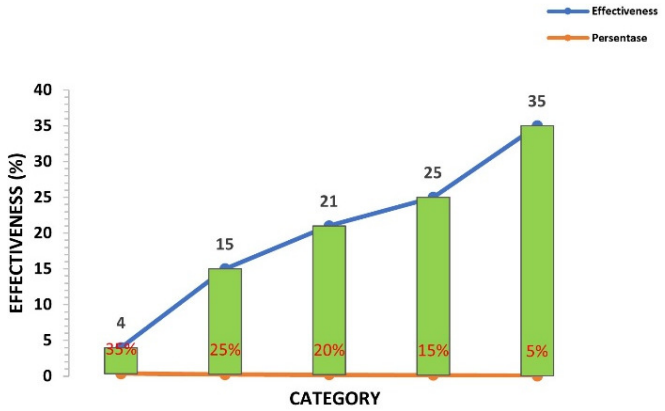

Fig. 9. Overheating protection effectiveness of the Metal Waste Cleaning-24 robot.

Figure 10 shows a comparison between the ANSYS simulation and experimental data. The simulation results show a fairly good level of accuracy with differences ranging from 0% to 20%. The deformation and stress parameters have high accuracy with differences below 7%, as well as roughness (5.9%), slippage (7.1%), and optimal weight (2.5%). However, there are more significant deviations in several parameters such as response time (20%), minimum stress (15%), and maximum volume (8%).

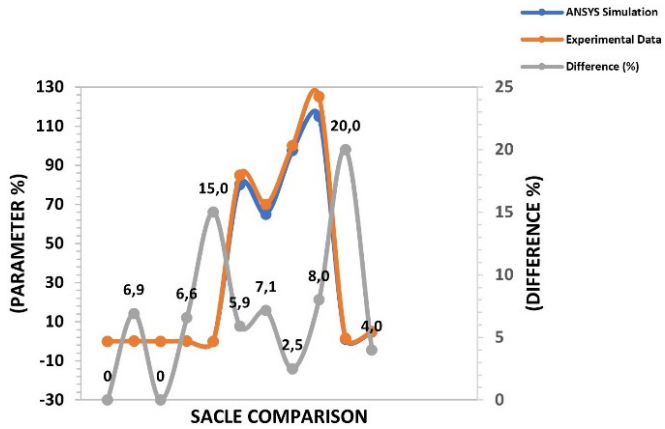

Fig. 10. Comparative analysis of the Metal Waste Cleaning-24 robot.

IV. CONCLUSION

The Metal Waste Cleaning-24 robot was successfully designed using an ESP32 microcontroller and a Proportional–Integral–Derivative (PID) controller with a sampling time of 10 ms. The robot is capable of handling metal waste with a capacity of 50-500 gr, maximum dimensions of 150 × 100 × 50 mm, and a material density of 2,000–8,000 kg/m^3. Aluminum alloy 319.0 exhibits a density of 2,796 kg/m^3, and a tensile strength of 246.1 MPa, with a maximum von Mises stress of 54.518 MPa observed in structural analysis. System validation shows that 60% of parameters meet the tolerance of ≤10%, with the highest accuracy achieved for minimum diameter (0% deviation) and the lowest accuracy within tolerance reaching 7.2%. Conversely, 40% of the parameters exceed the tolerance limit, with the highest deviations observed in response time (20.3%) and minimum stress (15.2%), indicating the need for system control optimization to achieve maximum performance in industrial metal waste cleaning operations.

The successful implementation of the PID control system with ESP32 microcontroller demonstrates the feasibility of low-cost, high-performance automation solutions for industrial waste management. The robot achieved a peak metal collection efficiency of 167 gr/min and a total recovered metal weight of 18,280 gr. These results have significant implications for industrial automation, offering potential reductions in occupational safety risks and operational costs while contributing to improved recycling efficiency and a reduced environmental impact of industrial metal waste.

Future research should prioritize addressing the identified performance limitations, particularly the 20.3% deviation in response time and 15.2% deviation in minimum stress, through advanced PID tuning methods such as genetic algorithms or particle swarm optimization. Medium-term research directions should focus on machine learning integration for adaptive control, multi-robot coordination capabilities for swarm robot applications, and expanding the system's capability to handle larger waste objects beyond the current 50–500 gr range. Long-term research should investigate hybrid control systems integrating neural networks with PID controllers, energy efficiency optimization through alternative energy sources, and development of modular designs for scalability across different industrial applications.

The current study presents preliminary findings that require further validation through extended field trials in diverse industrial environments. Limitations include the 10 ms sampling time and the simplified DC motor model, which may restrict performance in high-precision applications. Future work should include comprehensive long-term reliability testing, cost–benefit analyses across different industrial sectors, and the development of industry-specific customization protocols to maximize the practical impact of this technology in sustainable industrial waste management.

ACKNOWLEDGMENT

The authors would like to express their sincere gratitude to the editors and anonymous reviewers for their insightful comments and constructive suggestions, which greatly improved the quality and clarity of this manuscript. Their careful review and guidance played an important role in shaping the final version of this work. We would also like to thank the management and staff of the Mechatronics and Robotics Control Laboratory, Department of Mechanical Engineering, Hasanuddin University, for providing the research tools that enabled this work to be produced effectively for the benefit of the broader scientific community.

REFERENCES

[1] M.-W. Li, S.-M. Chang, and Y.-P. Liao, "Design and Implementation of a Cleaning Robot with Dual-Arms," in *2024 10th International Conference on Applied System Innovation*, Kyoto, Japan, 2024, pp. 15–17, https://doi.org/10.1109/ICASI60819.2024.10547771.

[2] A. Joon and W. Kowalczyk, "Design of Autonomous Mobile Robot for Cleaning in the Environment with Obstacles," *Applied Sciences*, vol. 11, no. 17, Sept. 2021, Art. no. 8076, https://doi.org/10.3390/app11178076.

[3] S. M. Saidi, R. Mellah, A. Fekik, and A. T. Azar, "Real-Time Fuzzy-PID for Mobile Robot Control and Vision-Based Obstacle Avoidance," *International Journal of Service Science, Management, Engineering, and Technology*, vol. 13, no. 1, pp. 1–32, Jan. 2022, https://doi.org/10.4018/IJSSMET.304818.

[4] X. Yu, Y. Fan, S. Xu, and L. Ou, "A self-adaptive SAC-PID control approach based on reinforcement learning for mobile robots," *International Journal of Robust and Nonlinear Control*, vol. 32, no. 18, pp. 9625–9643, Dec. 2022, https://doi.org/10.1002/rnc.5662.

[5] M. R. Razali, A. A. Mohd Faudzi, A. U. Shamsudin, and S. Mohamaddan, "A hybrid controller method with genetic algorithm optimization to measure position and angular for mobile robot motion control," *Frontiers in Robotics and AI*, vol. 9, Jan. 2023, Art. no. 1087371, https://doi.org/10.3389/frobt.2022.1087371.

[6] Z. Li, "Review of PID control design and tuning methods," *Journal of Physics: Conference Series*, vol. 2649, no. 1, Nov. 2023, Art. no. 012009, https://doi.org/10.1088/1742-6596/2649/1/012009.

[7] K. Zhu, "Optimization of Path Planning for Domestic Sweeping Robots Using Fuzzy PID Control," *Highlights in Science, Engineering and Technology*, vol. 111, pp. 590–596, Aug. 2024, https://doi.org/10.54097/22bk2502.

[8] M. A. U. F.A.B, "Rancang Bangun Robot Penghindar Halangan Dengan Metode PID," *Jurnal Teknik Mesin, Industri, Elektro dan Informatika*, vol. 2, no. 3, pp. 212–222, Aug. 2023, https://doi.org/10.55606/jtmei.v2i3.2352.

[9] V. Tinoco, M. F. Silva, F. N. Santos, R. Morais, S. A. Magalhães, and P. M. Oliveira, "A review of advanced controller methodologies for robotic manipulators," *International Journal of Dynamics and Control*, vol. 13, no. 1, Jan. 2025, Art. no. 36, https://doi.org/10.1007/s40435-024-01533-1.

[10] H. Meng, S. Zhang, W. Zhang, and Y. Ren, "Optimizing actual PID control for walking quadruped soft robots using genetic algorithms," *Scientific Reports*, vol. 14, no. 1, Oct. 2024, Art. no. 25946, https://doi.org/10.1038/s41598-024-77100-7.

[11] R. S. Ali, A. A. Aldair, and A. K. Almousawi, "Design an Optimal PID Controller using Artificial Bee Colony and Genetic Algorithm for Autonomous Mobile Robot," *International Journal of Computer Applications*, vol. 100, no. 16, pp. 8–16, Aug. 2014, https://doi.org/10.5120/17607-8016.

[12] M. I. Azeez, A. M. M. Abdelhaleem, S. Elnaggar, K. A. F. Moustafa, and K. R. Atia, "Optimization of PID trajectory tracking controller for a 3-DOF robotic manipulator using enhanced Artificial Bee Colony algorithm," *Scientific Reports*, vol. 13, no. 1, July 2023, Art. no. 11164, https://doi.org/10.1038/s41598-023-37895-3.

[13] M. Jasim Mohamed, B. K. Oleiwi, A. T. Azar, and A. R. Mahlous, "Hybrid controller with neural network PID/FOPID operations for two-link rigid robot manipulator based on the zebra optimization algorithm," *Frontiers in Robotics and AI*, vol. 11, June 2024, Art. no. 1386968, https://doi.org/10.3389/frobt.2024.1386968.

[14] J. Ito and Y. Wasa, "Data-Driven Adaptive PID Control Based on Physics-Informed Neural Networks." arXiv, Oct. 08, 2025, https://doi.org/10.48550/arXiv.2510.04591.

[15] A. Daniels, S. Kerz, S. Bari, V. Gabler, and D. Wollherr, "Grasping in Uncertain Environments: A Case Study For Industrial Robotic Recycling," in *2023 IEEE International Conference on Systems, Man, and Cybernetics*, Honolulu, Oahu, HI, USA, 2023, pp. 3514–3521, https://doi.org/10.1109/SMC53992.2023.10394008.

[16] A. G. Satav, S. Kubade, C. Amrutkar, G. Arya, and A. Pawar, "A state-of-the-art review on robotics in waste sorting: scope and challenges," *International Journal on Interactive Design and Manufacturing*, vol. 17, no. 6, pp. 2789–2806, Dec. 2023, https://doi.org/10.1007/s12008-023-01320-w.

[17] S. Ekinci, D. Izci, V. Gider, M. Bajaj, V. Blazek, and L. Prokop, "Quadratic interpolation optimization-based 2DoF-PID controller design for highly nonlinear continuous stirred-tank heater process," *Scientific Reports*, vol. 15, no. 1, May 2025, Art. no. 16324, https://doi.org/10.1038/s41598-025-01379-3.

[18] R. Shahouni, M. Bahraini, M. Abrofarakh, and M. Abbasi, "Adaptive tuning of fractional order PID controllers for nonlinear processes using hybrid PSO DQN reinforcement learning," *Scientific Reports*, vol. 15, no. 1, Nov. 2025, Art. no. 38545, https://doi.org/10.1038/s41598-025-22509-x.

[19] M. Likins, "Improve Process Efficiency Through Regulatory Control Stabilization." Yokogawa.

[20] "Recycling robots: Everything you need to know in 2025." Standardbots. https://standardbots.com/blog/recycling-robots-everything-you-need-to-know-in-2024.

[21] "Waste Sorting Robots Market Size, Value & Forecast to 2033." The Brainy Insights. https://www.thebrainyinsights.com/report/waste-sorting-robots-market-14094?srsltid=AfmBOookeJKXLSwiJN9rWHoU4kVtSN0fMVllHAEz6bYeb8lpR_pGCBAi.

[22] B. K. Oleiwi, M. Jasim, A. T. Azar, S. Ahmed, and A. R. Mahlous, "Bat optimization of hybrid neural network-FOPID controllers for robust robot manipulator control," *Frontiers in Robotics and AI*, vol. 12, May 2025, Art. no. 1487844, https://doi.org/10.3389/frobt.2025.1487844.

[23] K. Mendoza-Bautista, M. Alfaro-Ponce, and I. Chairez, "Hybrid robust disturbance rejection position-force control to adjust the motion of mobile manipulator in automatic aluminum foundry recycling industries," *International Journal of Sustainable Engineering*, vol. 17, no. 1, pp. 322–340, Dec. 2024, https://doi.org/10.1080/19397038.2024.2337787.

[24] J. Akl, Y. Patil, C. Todankar, and B. Calli, "Vision-Based Oxy-Fuel Torch Control for Robotic Metal Cutting," in *2023 IEEE/RSJ International Conference on Intelligent Robots and Systems*, Detroit, MI, USA, 2023, pp. 6403–6410, https://doi.org/10.1109/IROS55552.2023.10341532.

[25] *MakerbaseMoon/cleaner-4th-esp32*. (2025). Github. Accessed: Dec. 15, 2025. [Online]. Available: https://github.com/MakerbaseMoon/cleaner-4th-esp32

[26] Y. Wang, Y. Zhao, Y. Wu, S. Zhang, and J. Wang, "A Multi-sensor Intelligent Surface Garbage Cleaning Robot," in *2021 IEEE International Conference on Mechatronics and Automation*, Takamatsu, Japan, 2021, pp. 797–801, https://doi.org/10.1109/ICMA52036.2021.9512614.

[27] "Waste Sorting Robots Market Size, Share & Growth, 2033." Market Data Forecast. https://www.marketdataforecast.com/market-reports/waste-sorting-robots-market.

[28] R. R. Kundavaram, A. R. Onteddu, K. Devarapu, D. Narsina, and M. Nizamuddin, "Advances in Autonomous Robotics for Environmental Cleanup and Hazardous Waste Management," *Asia Pacific Journal of Energy and Environment*, vol. 12, no. 1, pp. 1–16, Feb. 2025, https://doi.org/10.18034/apjee.v12i1.788.

[29] N. Naajihah Ab Rahman and N. Mat Yahya, "System Identification for a Mathematical Model of DC Motor System," in *2022 IEEE International Conference on Automatic Control and Intelligent Systems*, Shah Alam, Malaysia, 2022, pp. 30–35, https://doi.org/10.1109/I2CACIS54679.2022.9815461.

[30] N. N. A. Rahman and N. M. Yahya, "A mathematical model of a brushed DC motor system," *Data Analytics and Applied Mathematics*, vol. 2, no. 2, pp. 60–68, Dec. 2021, https://doi.org/10.15282/daam.v2i2.6830.

[31] A. Hoang, S. T. Nguyen, T. V. Pham, T. M. Pham, L. V. Trieu, and T. T. Cao, "A Bayesian Neural Network-based Obstacle Avoidance Algorithm for an Educational Autonomous Mobile Robot Platform," *Engineering, Technology & Applied Science Research*, vol. 13, no. 6, pp. 12183–12189, Dec. 2023, https://doi.org/10.48084/etasr.6304.

[32] M. Kuczmann, "Review of DC Motor Modeling and Linear Control: Theory with Laboratory Tests," *Electronics*, vol. 13, no. 11, June 2024, Art. no. 2225, https://doi.org/10.3390/electronics13112225.

[33] F. Ding, "Finite element analysis and optimal design of robotic arm," *Applied and Computational Engineering*, vol. 33, pp. 88–93, Feb. 2024, https://doi.org/10.54254/2755-2721/33/20230238.

[34] X. Li and J. Liang, "Optimization design and finite element analysis of welding robot base based on ANSYS Workbench," *Journal of Physics: Conference Series*, vol. 2383, no. 1, Dec. 2022, Art. no. 012073, https://doi.org/10.1088/1742-6596/2383/1/012073.

[35] J. Zhang, L. Wang, and L. Jing, "Static Analysis of Manipulator Based on Solidworks and ANSYS Workbench," *Journal of Physics: Conference Series*, vol. 2477, no. 1, Apr. 2023, Art. no. 012099, https://doi.org/10.1088/1742-6596/2477/1/012099.

[36] N. Khedkar, K. Wani, V. Jatti, and V. Joshi, "Experimental, Modal, and Harmonic Response Analysis of a Chladni Plate at Ultrasonic Frequencies," *Engineering, Technology & Applied Science Research*, vol. 13, no. 6, pp. 12289–12294, Dec. 2023, https://doi.org/10.48084/etasr.6428.

[37] M. R. Sagita, A. Ma'arif, F. Furizal, C. Rekik, W. Caesarendra, and R. Majdoubi, "Motion System of a Four-Wheeled Robot Using a PID Controller Based on MPU and Rotary Encoder Sensors," *Control Systems and Optimization Letters*, vol. 2, no. 2, pp. 257–265, Nov. 2024, https://doi.org/10.59247/csol.v2i2.150.

[38] Y. Zheng, M. Liu, B. Li, G. Ma, and M. Xiao, "Structural optimization of a pipe-climbing robot based on ANSYS," *Mechanical Sciences*, vol. 13, no. 2, pp. 725–733, Aug. 2022, https://doi.org/10.5194/ms-13-725-2022.

[39] N. T. Minh Nguyet and D. X. Ba, "A neural flexible PID controller for task-space control of robotic manipulators," *Frontiers in Robotics and AI*, vol. 9, Jan. 2023, Art. no. 975850, https://doi.org/10.3389/frobt.2022.975850.

[40] O. Çakar and M. Alçın, "Industrial robot arm analysis using finite element method," *Bilgisayar Bilimleri ve Teknolojileri Dergisi*, vol. 3, no. 1, pp. 30–37, Aug. 2022, https://doi.org/10.54047/bibted.1111400.

[41] J. Yu, K. Yang, S. Chen, and J. Zhang, "Lightweight Design of Heavy-duty Logistics Robot Based on ANSYS," *Academic Journal of Science and Technology*, vol. 10, no. 2, pp. 26–31, Apr. 2024, https://doi.org/10.54097/0t6m7f71.

[42] F. Alhajri and H. Ali Alajmi, "Finite Element Analysis and Design Optimisation of Welding robot base using ANSYS," *International Journal of Innovative Science and Research Technology*, vol. 9, no. 9, pp. 3424–3430, Sept. 2024, https://doi.org/10.38124/ijisrt/IJISRT24SEP877.

[43] X. Yang, C. Zhang, and L. Zhou, "Static analysis and optimization design of a special-shaped rod of the crab-like robot based on ANSYS Workbench," *Journal of Physics: Conference Series*, vol. 2459, no. 1, Mar. 2023, Art. no. 012136, https://doi.org/10.1088/1742-6596/2459/1/012136.

[44] T. D. Phan *et al.*, "Research Impact of Solar Panel Cleaning Robot on Photovoltaic Panel's Deflection." arXiv, June 09, 2023, https://doi.org/10.48550/arXiv.2306.05340.

AUTHORS PROFILE

La Ode Muhammad Ali is a graduate student in Mechanical Engineering at Hasanuddin University, specializing in machine construction. This is his second research publication. Email: ldmuhammadali@gmail.com

Andi Amijoyo Mocthar is a researcher and lecturer in Mechanical Engineering at Hasanuddin University, serving as the first supervisor. Email: andijoyo@unhas.ac.id

Fauzan Djamaluddin is a researcher and lecturer in Mechanical Engineering at Hasanuddin University, serving as the second supervisor. Email: fauzan@unhas.ac.id